ICAF

International Committee on Aeronautical Fatigue and Structural Integrity

ICAF

Review of Aeronautical Fatigue Investigations in Germany during the Period of April 2023 - March 2025

Abstract

This review represents a compilation of abstracts on aeronautical fatigue investigations in Germany during the period from April 2023 - March 2025. It will be published on the ICAF website, as well. The contribution of summaries by German aerospace manufacturers, governmental and private research institutes, universities as well as aerospace authorities was voluntary, and is acknowledged with sincere appreciation by the author of this review. Enquiries concerning the individual contents shall be addressed directly to the author of the corresponding summary.

HOMBERGSMEIER, Elke

elke.hombergsmeier@airbus.com

Contents

1. Introduction

This review represents a compilation of abstracts on aeronautical fatigue investigations in Germany during the period from April 2023 - March 2025. It will be published on the ICAF website https://www.icaf.aero/ and presented during the ICAF 2025 – the 39th Conference and 32nd Symposium of the International Committee on Aeronautical Fatigue and Structural Integrity. All related information is available on the ICAF 2025 Website https://www.icaf2025.com

The contribution of summaries by German aerospace manufacturers, governmental and private research institutes, universities as well as aerospace authorities (Table 1) was completely voluntary, and is acknowledged with sincere appreciation by the author of this review.

Enquiries concerning the individual contents shall be addressed directly to the author of the corresponding summary.

Table 1: Overview of contributing companies and institutes

Abbreviation	Details
AIRBUS CRT	Airbus Central Research & Technology, Willy-Messerschmitt-Strasse 1, 82024 Taufkirchen, Germany, www.airbus.com
HZH	Institute of Materials Mechanics and Institute of Materials Physics, Helmholtz-Zentrum Hereon, Max-Planck-Str. 1, 21502 Geesthacht, Germany www.hereon.de
IVW	Leibniz-Institut für Verbundwerkstoffe GmbH, Erwin-Schrödinger-Str. 58, 67663 Kaiserslautern, Germany, www.ivw.uni-kl.de
PPI	Institute for Production Technology and Systems, Leuphana University of Lüneburg, Universitätsallee 1, 21335 Lüneburg, Germany, www.leuphana.de/en/institutes/ppi.html

2. ADVANCED MATERIALS, PROCESSES AND INNOVATIVE STRUCTURES

2.1. Impact of powder feedstock quality on directly L-PBF generated AlSi7Mg0.6 (F357) material

Frank Palm (Airbus Central Research & Technology)
Contact: frank.palm@airbus.com

Additive manufacturing, in particular laser powderbed fusion (L-PBF), is exciting aerospace engineers because it enables extraordinary design solutions which can save weight in strength as well as functionally driven parts (“topology optimization”). However its propensity (and big difference to classically designed & manufactured parts) of direct material creation in combination with the 3D-part production sacrifices one important pillar of aerospace safety ⇒ **The control and related confidence in the basic material properties which are used to develop and deduce a reliable part designs with sufficient load bearing capabilities.**
In established manufacturing procedures the Certificate of Conformity of the material producer or supplier assures the material (strength) properties. In 3D-printing processes like L-PBF the part material is the directly generated product from a complex laser-based interaction of a powder feedstock, the conversion of laser energy (beam) powder into (local) heat which melts the substrate as well as the powder using tailored scan pattern to reach a required full coverage of a predefined 2D-layer. Consequently, layer by layer you incrementally create a more or less dense part (and material) defining the directly created material and part properties (with a significant amount of uncertainties).

Many process parameters along this sophisticated direct manufacturing approach tend to be notoriously unstable. In particular, the laser energy conversion process discloses in combination with Aluminum alloys many peculiarities resulting in a strong fluctuation of process heat which can cause difficulties to master melt puddle dynamics leading to a bunch of strength-critical imperfections like voids, pores or other features. More so L-PBF parameter developing campaigns proved that also Aluminum powders inherent processability like flow behaviour but even more its metallurgical cleanliness (potential contamination with hydrogen and oxygen (oxide)) can be of major concern w.r.t the final 3D-printed part performance.

Case study: The presented data (static strength & fatigue (R= 0.1)) summarize an extended investigation done with the investment cast type popular aerospace Al-alloy F357 (AlSi7Mg0.6 (Beryllium-free)). Due to its very good castability it is also ideally suited for L-PBF processing and can deliver persuading high strength values (> 400 MPa) exceeding those of investment cast parts by 20%. However the material requires tailored post L-PBF process heat treatments to assure an

appropriate combination of UTS / YS and fracture elongation (depending on part application). It becomes obvious that the powder quality seems to trigger directly the L-PBF and post-L-PBF heat treatment process schemes. Hence it was decided to investigate the impact of 2 different (commercially available) F357 powders: Type "A" was a high quality variant which offers a "clean" material composition and a "full" spherical powder morphology whereas the 2nd powder Type "B" represented a standard powder quality (i.e. often supplied by many L-PBF platform manufacturers). Table 2 summarizes the 2 different powders and highlights the main differences (hydrogen and oxygen content as well powder particle morphology). 3 different post-L-PBF heat treatments were defined:

I. A short time low temperature stress relief which might also enable some precipitation hardening in the F357 material matrix (⇒ 220°C/15 min. in pre-heated liquid oil).
II. An established T6 temper treatment (based on aerospace standards for investment cast F357 type material but with reduced durations to avoid too strong grain coarsening) using lab air furnaces.
III. A microstructure repair (post-L-PBF "densification") by running a HIP process step followed by T6 temper (HIP was done with Argon).

Table 2: Summary information about both F 357 powder variants and post-L-PBF process heat treatments

Powder A (a/b/c)		**Powder B** (e/f/g)	
Feedstock: Industrially produced ingot ⇒ cast ⇒ extruded into 60 mm rods / Ar-atomization		Feedstock: Arranged by powder manufacturer from own (unknown = non specified) sources / N2-atomization	
Oxygen	206 ppm	Oxygen	381 ppm
Hydrogen	**2 ppm**	**Hydrogen**	**18 ppm**
Flowability/Spreadability	excellent	Flowability/Spreadability	very good
LPBF-process parameter: Medium build-rate ⇒ ~ 30 cm³/h followed by 3 different post LPBF heat treatments			
Direct aging & low temperature residual stress annealing			220°C / 15 min. / liquid bath
Spec. acc. high temperature solution heat treatment / WQ / artificial aging			540°C / 2h / WQ / 175°C / 6h (furnace - in air)
HIP densification + High temperature solution heat treatment / WQ / artificial aging		520°C / 2h / 1000 bar / FC (Ar-HIP)	540°C / 2h / WQ / 175°C / 6h (furnace - in air)

Static strength testing of all testbodies have been done with machined dog-bone type samples in acc. to DIN EN ISO 6892-1. Figure 1 exhibits a summary of all strength test measurements. Powder A and powder B both treated with the low temperature annealing, revealed comparable UTS and YS values; however the more "dirty" powder B based F357 showed some deficits on material plasticity.

Case study - LPBF of AlSi7Mg0.6 (F357)

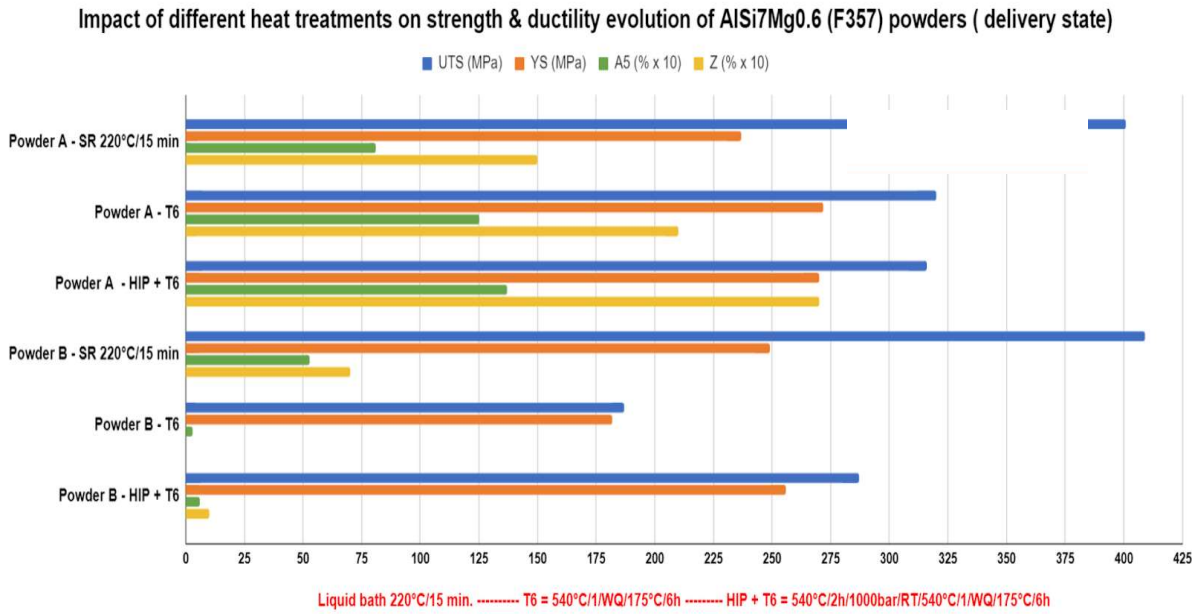

Figure 1: Strength evolution in F357 type material (L-PBF of 2 different Al-powders + 3 different heat treatments)

The T6 temper modifies the 3D-printed microstructures in F357 drastically. The original rapidly solidified very fine structured eutectic Al-Si cell structure overlaid with nano-sized primary Si-particles disappeared completely and was replaced by a homogenized coarse grained Al-Si lattice where primary (incoherent) & secondary Mg_2Si (coherent) determines strength & ductility. However the high solutionizing temperature of about 540°C dramatically mobilized the hydrogen already trapped in the F357 powder (especially powder B) and now present in the generated bulk material. Such atomic hydrogen recombines into molecular hydrogen gas and “pearls out” overall in the material in particular for powder B damaging the related bulk material significantly (s. also Figure 4). Consequently, powder B creates inferior strength and much more ductility losses compared to powder A. Even the HIP based L-PBF post process was not able to restore (partially) the material strength capabilities. But for powder A HIP could further improve the actually satisfying static material property mix.

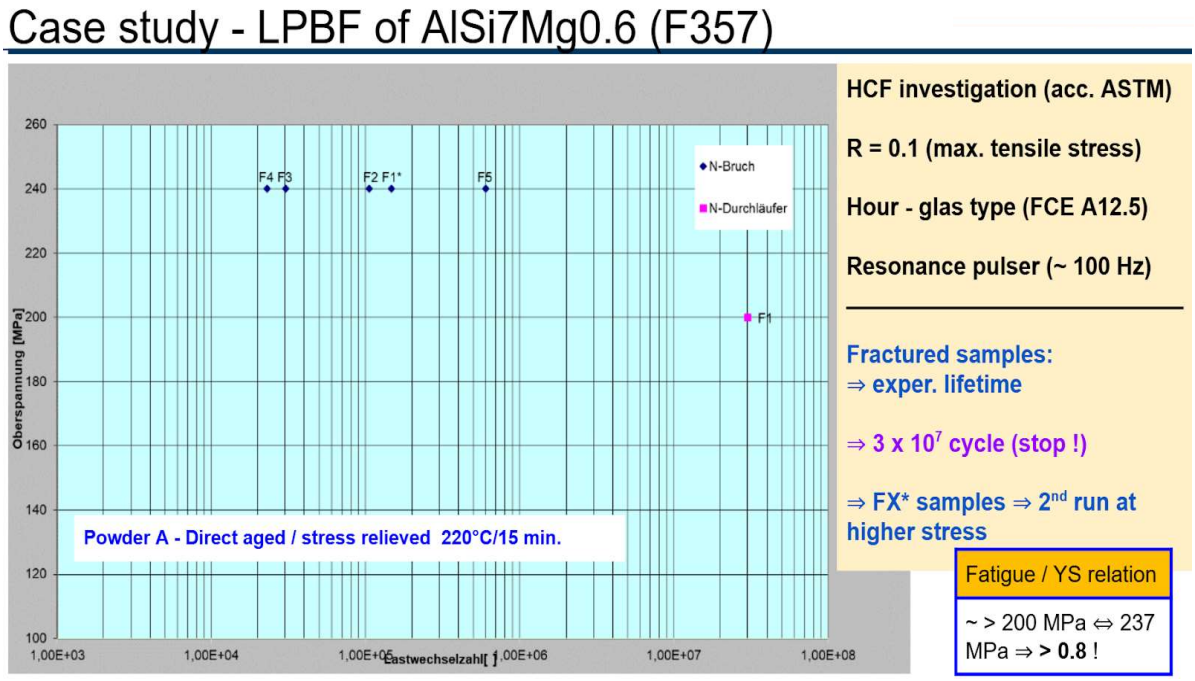

Figure 2: Cyclic strength durability of F357 in temper condition I (powder A)

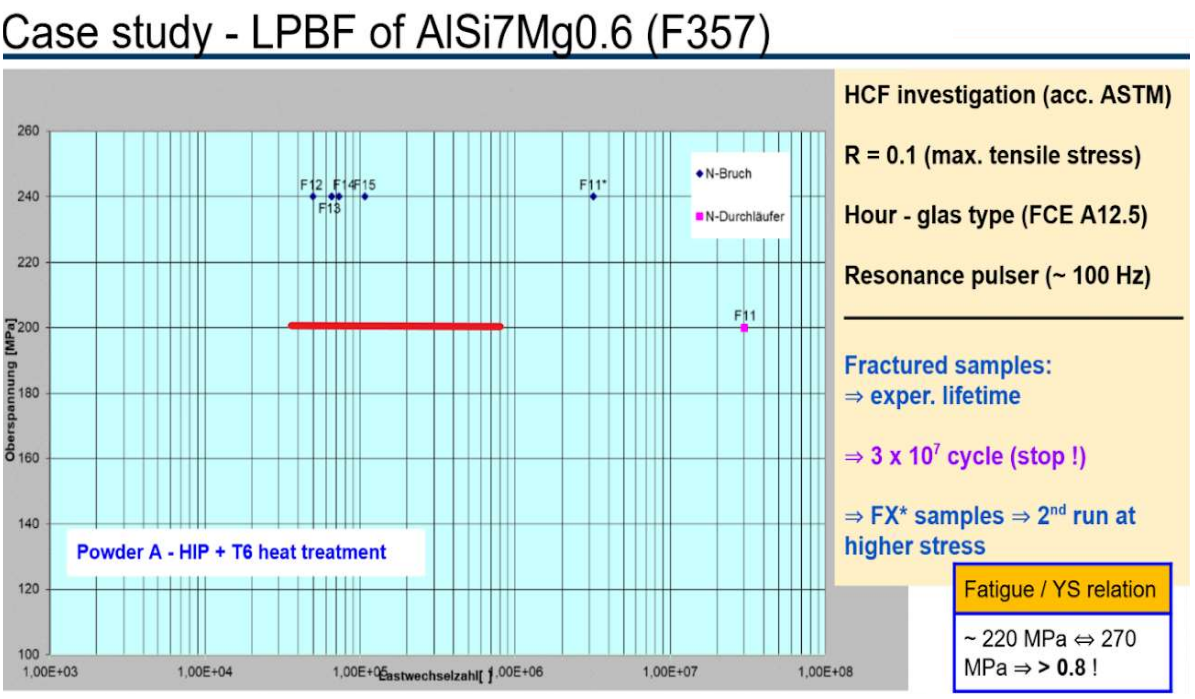

Figure 3: Cyclic strength durability of F357 in temper condition III (powder A) ⇒ red bar refers to the fatigue results of 5 test samples with a sole T6 heat treatment (no HIP !) condition II

After testing the hourglass-shaped (FCE-A12.5) fatigue samples, very good durability properties were recorded for the liquid bath short-term heat treated powder A material (Fig. 2 and 3). Equivalent results were possible for powder A if the T6 temper is combined with HIP treatment. A sole T6 process revealed for both powders weakening effects, though the higher hydrogen "packed" powder B is suffering extremely (in static (Fig. 1) as well fatigue performance (not displayed in this ICAF summary). Exemplarily the "T6 time strength window at 200 MPa max. upper stress" values of "clean" powder A are depicted as a red horizontal bar in Figure 3. Microstructure repair enabled by HIP for powder A is shifting up these values by more than 20% (⇒ 240 MPa) because at 200 MPa we observed run-outs at 30 x 10^6 cycles. The relation between fatigue strength and max. yield strength (YS) exceeds the factor of 0.5 significantly. Surprisingly, such high intrinsic fatigue properties of the 3D-printed material outperforms established premium investment cast material F357 HCF data by more than 30% (an unexpectedly good material peculiarity if you compare this with incumbent static - cyclic strength ratios in wrought high performance aerospace Al-alloys like 2024 or 7075).

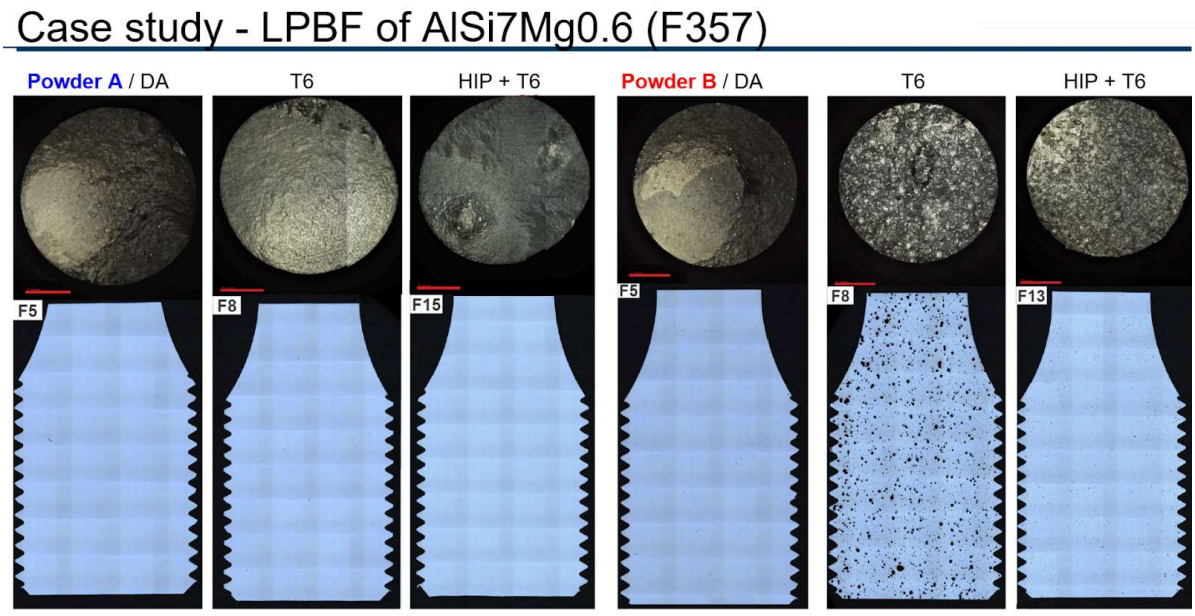

Figure 4: "Post mortem" failure investigation of fatigue sample densities originating from powder A and powder B ⇒ see high porosity by T6 temper in L-PBF material from powder B

State of the art aerospace materials are almost free of hydrogen (< 1 ppm) and very rarely contaminated with oxide. This is secured due appropriate melt material treatments like Ar-flushing (⇒ to remove the hydrogen) and 3-step-filtering during slab- or billet pouring (to hold back melt surface oxide skins). Hence, any high temperature heat treatment to homogenize, solutionize and recrystallize the microstructure can be readily done without sacrificing the later material property portfolio (i.e. uncontrolled hydrogen porosity evolution). Directly generated

(additively manufactured) materials are always reflecting the quality of the used feedstock either powder or wire (Fig. 4). In particular the currently established way to manufacture Al-powders for 3D-printing is unfortunately not taking care about decades of lessons learnt from classical Aluminum semi-product manufacturing. Non-removed hydrogen contaminations beyond 15 - 20 ppm in the Al-alloy melt prepared for atomization can later cause very detrimental effects after L-PBF as well post-process heat treatments penalizing desired quality and required reliability drastically. Derived from these and other investigation data there seems to be a process window of < 5 ppm hydrogen in L-PBF for Al-alloys where a high(er) degree of process robustness is possible. W.r.t. the oxygen (or better said oxide) contamination there are still remaining questions about how those oxides could appear (particles, agglomerates, skins etc.). However also here it is without contradiction that minimizing the global amount of oxide in general will be beneficial. We see < 500 ppm as a 1st step but it should finally be possible to secure < 150 - 200 ppm in a tailored L-PBF Aluminum powder.

There are 2 clear messages deducible from the presented investigations:

- ➢ L-PBF process propensities as well as strength - ductility properties become more reliable at higher strength level when the hydrogen contamination of Al-powders is low (< 5ppm) creating more trustworthiness in this new manufacturing scheme.
- ➢ Astonishingly high static strength ⇔ fatigue properties in F357 are possible provided that the amount microstructure imperfections (incl. contaminations) are low ⇒ HIP can help to restore material static & cyclic durability (but be aware that material fatigue capabilities and part durability (load bearing capabilities) are different topics).

2.2. Identification of Johnson-Cook Material Model Parameters for Laser Shock Peening Process Simulation

R. Kuliiev, S. Keller, and N. Kashaev (Helmholtz-Zentrum Hereon)
Contact: nikolai.kashaev@hereon.de

Laser Shock Peening (LSP) is a proven surface engineering technique for enhancing the fatigue, corrosion and wear resistance of metallic materials. LSP uses high-intensity (in GW/cm^2 range) and low-duration laser pulses (usually less than 50 ns) to introduce high depth-resolved compressive residual stresses on the component by means of a laser-induced high-pressure wave resulting from plasma expansion. The shock wave generated during this process propagates through the workpiece, causing plastic deformation and simultaneously inducing the residual stress field. Once the laser pulse ends, the plasma dissipates and is no longer able

to generate high pressure to induce the shock wave. Applying a thin water layer prevents plasma dissipation, increases the surface's exposure to high pressure, and limits plasma expansion away from the surface (towards the laser beam). This results in a pressure pulse length that is up to five times longer than the laser pulse duration and a maximum or peak pressure that is up to 10 times higher than the LSP process without the applied confinement layer. The depth-resolved compressive residual stresses after LSP application can be generated up to several millimetres deep, which is significantly higher than the typical depth of 300 µm achieved by industrially established processes such as shot penning.

The scientific community has thoroughly researched the impact of the LSP process on the generation of residual stress fields in engineering metallic materials, along with the enhancement of their fatigue life. However, developing a reliable model to predict material behaviour during LSP application remains challenging. Finite element analysis (FEA) is a widely employed method to develop such a model. It simulates the mechanical effect of a laser pulse on the material by applying a time-dependent pressure profile to cause plastic deformation and incorporate the residual stresses through the depth of the component. Nevertheless, certain uncertainties are associated with the model, including the accuracy of the shape of the pressure profile for each LSP shot; the maximum value of the pressure as well as an LSP shot duration. Furthermore, the accurate determination of material model parameters, particularly in the context of accommodating strain rates ranging from 10^6 to 10^7 s^{-1}, poses a notable challenge in material response simulation after the LSP application.

The Johnson-Cook (JC) material model is a widely utilised approach for simulating high strain rate processes, such as LSP. It incorporates considerations of material hardening behaviour in addition to the strain rate dependency of the material, thus ensuring its extensive utilisation in LSP simulations. The determination of JC material model parameters necessitates the execution of tensile or compressive experiments at various strain rates, encompassing both quasi-static and high strain rates up to 10^4 s^{-1}. These experiments can be performed utilising a Split-Hopkinson pressure bar, also designated as a Kolsky bar. However, it is imperative to acknowledge that conducting experiments at elevated testing strain rates may introduce challenges that can compromise the quality of the obtained data. The presence of artefacts induced by the loading device during stress-strain data measurements can lead to inaccuracies in the identification of JC material model parameters, potentially misrepresenting the material's actual behaviour. Consequently, the substantial variability in JC material model parameters observed across different research articles, even for the same material, underscores the necessity to address this issue.

To address the challenges described above, the present study focuses on the identification of parameters of the JC material model for the simulation of high strain rate processes such as LSP [1]. A combined numerical and experimental approach is used to identify the material parameters for the alloys AA2024-T3, Ti-6Al-4V and Inconel 718. The experimental approach consisted of controlled impacts with an indenter at different velocities (Fig. 5a-c), allowing a detailed study of the reaction dynamics of the material and an evaluation of the resulting surface deformations. To validate the parameters, the depth resolved residual stress profiles are evaluated after the experimental and numerical application of LSP (Fig. 5d). The results showed excellent agreement between the experimental and numerical behaviour of AA2024-T3 and Inconel 718, indicating the high reliability of the identified Johnson-Cook parameters for these alloys. However, the strain rate-dependent coefficient C of the JC model determined at low strain rates is not sufficient to accurately describe the behaviour of the Ti-6Al-4V alloy. It is therefore necessary to identify and determine an appropriate parameter C of the JC model, specifically tailored to the strain rates relevant to the intended application of the material. The results of this study provide important insights into the accurate identification of the parameters of the JC material model for laser shock peening simulations. Overall, the developed approach has been validated through a series of experiments and simulations, demonstrating its applicability to both low and high strain rate processes, particularly in the context of LSP.

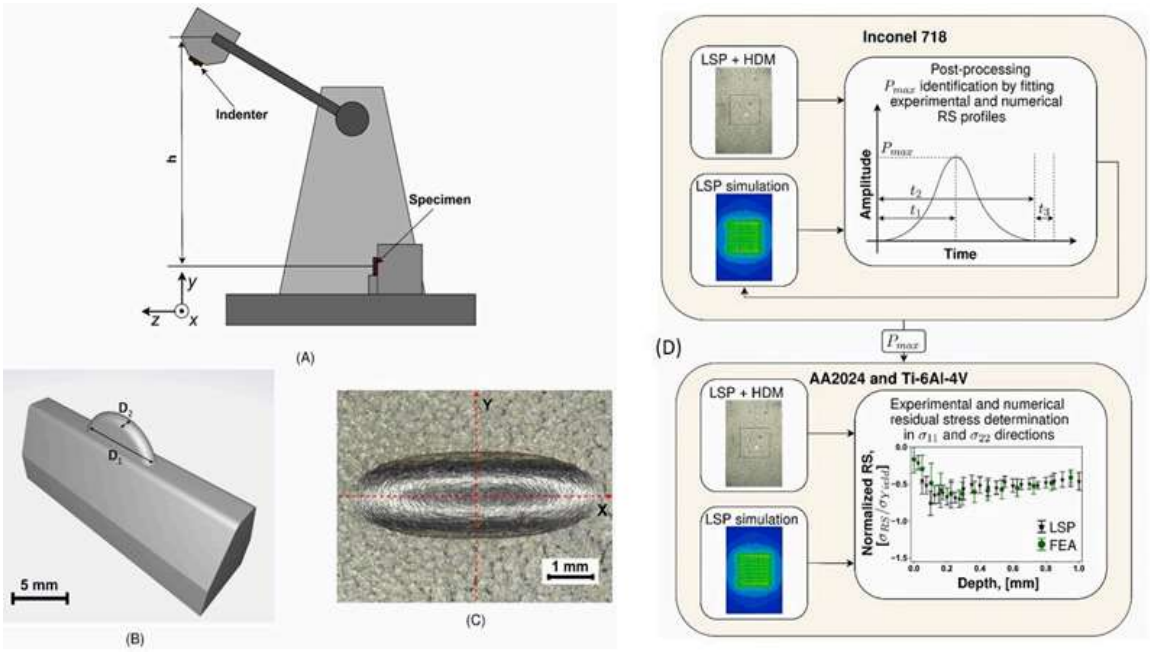

Figure 5: a) A schematic of a Charpy testing machine, b) fabricated impact indenter, c) an example of the im-pact region on Inconel 718, and d) a diagram of the validation process of the JC material model parameters. HDM and FEA denote the incremental hole drilling method for the RS analysis and finite element analysis, respectively.

References

[1] R. Kuliiev, S. Keller, N. Kashaev. Identification of Johnson-Cook material model parameters for laser shock peening process simulation for AA2024, Ti–6Al–4V and Inconel 718. Journal of Materials Research and Technology 2024; 28: 1975–1989.

3. Fatigue life enhancement methods and repair solutions

3.1. Application of Laser Shock Peening as a Manufacturing and Repair Process to Improve the Fatigue Performance of Refill Friction Stir Spot-welded AA2024 Joints

N. Kashaev[1], T. Mohr[1], S. Keller[1], U. F. H. Suhuddin[1], B. Klusemann[1,2], F. Dorn[1], V. Ventzke[1]
([1]Institute of Material and Process Design, Helmholtz-Zentrum Hereon)
([2]Institute for Production Technology and Systems, Leuphana University of Lüneburg)
Contact: nikolai.kashaev@hereon.de

The traditional way of joining thin-walled aluminum structures in aircraft construction is by riveting. A hole must be drilled to insert a rivet. During aircraft operation, fatigue cracks from the drilled holes can be developed because of cyclic loading. Stress amplification at the holes may accelerate fatigue crack initiation and growth. With refill Friction Stir Spot Welding (refill FSSW), the Helmholtz-Zentrum Hereon has patented an innovative manufacturing process that has the potential to replace rivets in aircraft construction [1]. The refill FSSW process has evolved from classic friction stir welding, which is already used in the aerospace industry. As a solid-state joining process, refill FSSW requires no filler material and can join difficult-to-weld materials such as high-strength aluminum alloys. Compared to riveting, the process has the advantage of avoiding stress concentration by eliminating holes. In addition, weight can be saved compared to riveting. These properties make refill FSSW a possible alternative to riveting in the aerospace sector. However, the use of structural weldments always presents a significant challenge for implementation in a damage tolerant design, where a complete understanding of crack initiation and growth is essential for the application of refill FSSW in the aerospace industry. In this context, the fatigue strength of refill FSSW joints under cyclic loading is only 15% of the ultimate lap shear strength [2], which is lower compared to the value of 22% for standard riveted joints [3].

To address this challenge, Laser Shock Peening (LSP) is investigated as an innovative residual stress engineering technique to improve the fatigue performance

of refill FSSW AA2024-T3 joints [4]. To this end, fatigue tests were carried out on specimens joined in an overlap configuration by refill FSSW (Fig. 6a) and on specimens subsequently treated with LSP on one side (Fig. 6b) and on both sides (Fig. 6c). The LSP treatment was applied to an area of 18 mm × 18 mm. The area was treated twice with LSP using a square laser spot of 1 mm × 1 mm. The laser energy was set at 3 J, resulting in a power density of 15 GW/cm^2 for a constant laser pulse duration of 20 ns (full width at half maximum). For the LSP treatment, the material surface was covered with a laminar layer of water, which was used as a confinement medium for the plasma. No ablative layer was used.

The uniaxial fatigue tests were performed using a 10 kN servo-hydraulic testing machine at a frequency of f ≈ 20 Hz, a constant load ratio of 0.1 and at room temperature. The fatigue test results as a function of the maximum cyclic load F_{max} on the number of cycles to failure were analyzed using the Basquin equation [5] to calculate the 10%, 50% and 90% survival probabilities and the Basquin fatigue strength at 2 × 10^6 cycles.

Two application scenarios are investigated, one investigating the LSP technique as a complementary manufacturing process to the refill FSSW technology (Fig. 6d), and the other investigating the LSP technique as a repair process for damaged joints (Fig. 6e). The fatigue test results showed that the application of the LSP treatment can significantly improve the fatigue behavior of the refill FSSW overlap joints. In terms of Basquin fatigue strength, the LSP treatment resulted in an improvement by a factor of 1.51 and 2.82 for the one- and two-sided LSP-treated specimens, respectively (Fig 6d). The life of specimens with refill FSSW joints that had been specifically pre-damaged by stopping the fatigue test at approximately 50%, 75% and 83% of the number of cycles to the Basquin fatigue strength of 2 × 10^6, applying LSP treatment and continuing the fatigue test was also significantly extended (Fig. 6e).

The results of this study show that LSP is a very effective technique for significantly extending the fatigue life of refill FSSW joints. Therefore, the combination of these two manufacturing processes, refill FSSW and LSP, represents a promising technology for industrial companies that require high fatigue performance for their structural components.

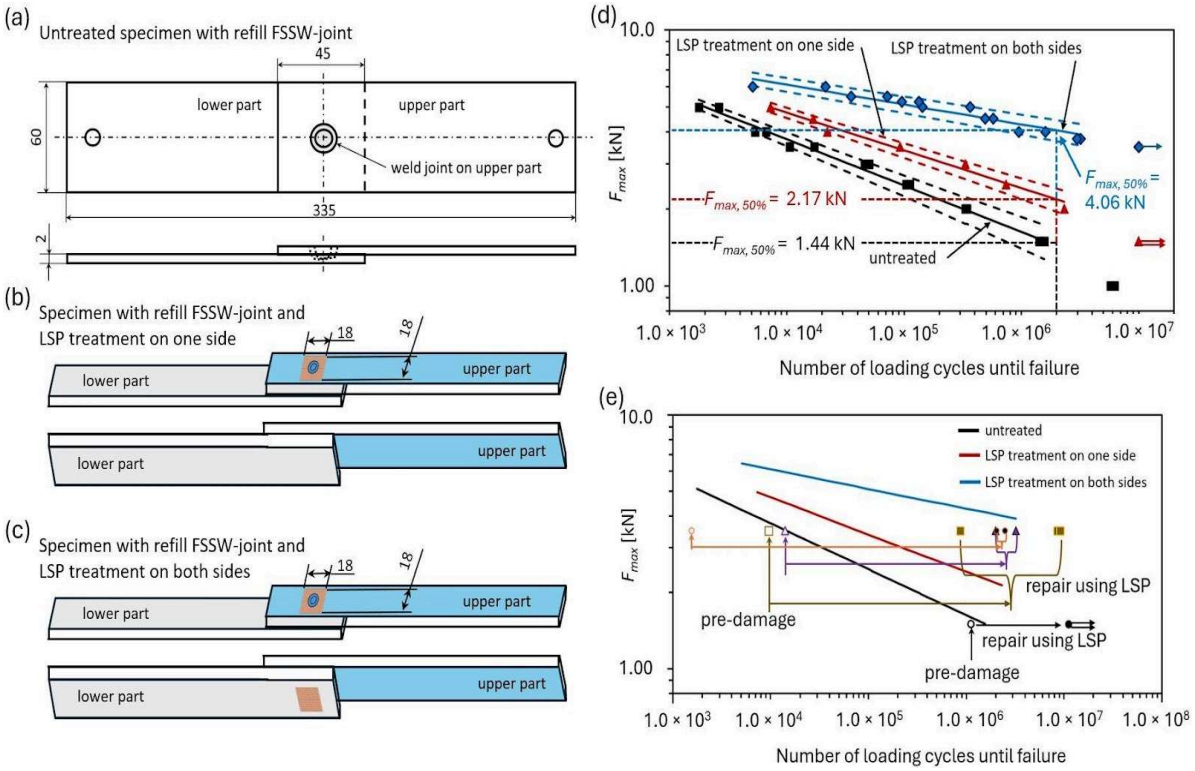

Figure 6: (a)-(c) Geometry of specimens used for fatigue tests: (a) untreated specimen with refill FSSW-joint, (b) specimen with refill FSSW-joint and LSP treatment on one side, and (c) specimen with refill FSSW-joint and LSP treatment on both sides. All dimensions are in mm. (d) Fatigue test results of untreated and LSP treated specimens. Also shown is the 50% failure probability and the 10% and 90% failure probabilities for each configuration. (e) Results of fatigue testing of pre-damaged specimens after LSP treatment on both sides. The diagram shows the 50% failure probabilities for the three configurations tested and the specimen positions where the fatigue tests were interrupted and continued with the same specimen after LSP treatment.

References

[1] C. Schilling, J. dos Santos. Method and device for joining at least two adjoining work pieces by friction welding. US Patent No. US 6,722,556 B2. 2004.

[2] R. C. Brzostek, U. Suhuddin, J.F. dos Santos. Fatigue assessment of refill friction stir spot weld in AA 2024-T3 similar joints. Fatigue Fract. Eng. Mater. Struct. 41(5) (2018) 1208-1223.

[3] N. Kashaev et al. Development of laser beam welding concepts for fuselage panels. 5th CEAS Air & Space Conference, 2015. Paper No. 15.

[4] N. Kashaev, B. Klusemann et al. Component with spot-welded lap joints. European Patent. File Number: EP 4438216. Publication Date: 02.10.2024.

[5] J. Schijve. Fatigue of Structures and Materials. 2nd ed. Delft: Springer. 2009.

3.2. Correlation of fatigue damage with polymer and microstructural parameters in thermoplastic tapes and epoxy resin with non-crimp fabric reinforcement

Andreas Baumann and Joachim Hausmann (IVW – Leibniz-Institut für Verbundwerkstoffe)
Contact: Andreas.Baumann@ivw.uni-kl.de

Fatigue qualification of continuous fiber reinforced materials is one of the first building blocks required in the test pyramid [1]. A major benefit of coupon level characterization is a limited testing effort allowing for the investigation of a broad range of load ratios and stress levels. A transition from coupon to component testing introduces uncertainties, due to variations in processing parameters and potential defects. To account for this, coupon level testing will typically be supplemented by additional structural element testing to account for local specifics [1], like open or filled holes. This approach already recognizes uncertainties when moving to the next level of the building block.

In light of this, a recent study on the most basic building blocks of composite components was undertaken to foster a deeper understanding of the constituent effect. Due to the experimental techniques employed for fatigue testing the influence of the geometric arrangement on a sub-ply level (i.e., arrangement of rovings or fiber clusters) could be identified, too. From the three main constituents, the focus was on the polymer effect on fatigue. For this a detailed study of the polymer properties of bisphenol-A based polycarbonate and epoxy resin (Rim 135 / Rimh 137) in two molecularly modified states was correlated to the fatigue performance of their laminates with carbon and glass fiber reinforcement. A modification of the polymers without alterations of the fiber arrangement was achieved by exposing both, the polymer specimens and the laminates, to γ-rays (Cobalt 60 source) as a post-cure treatment. Both polymers were chosen to consider their measurable response to irradiation treatment and not from an application's perspective.

In the following, two aspects relevant to the testing pyramid will be discussed. First, the uncertainty introduced by the fiber arrangement and second, the effect of varied polymer properties on the fatigue damage within a laminate. The analyzed loading scenario is transverse tension-tension loading (R = 0.1) as part of a cross-ply lay-up $[90_n/0]_s$. The lay-up allows for the formation of multiple transverse cracks and avoids that one of them becomes preliminarily critical and ends the test by sudden failure. The latter is typical for unidirectional transversely loaded laminates.

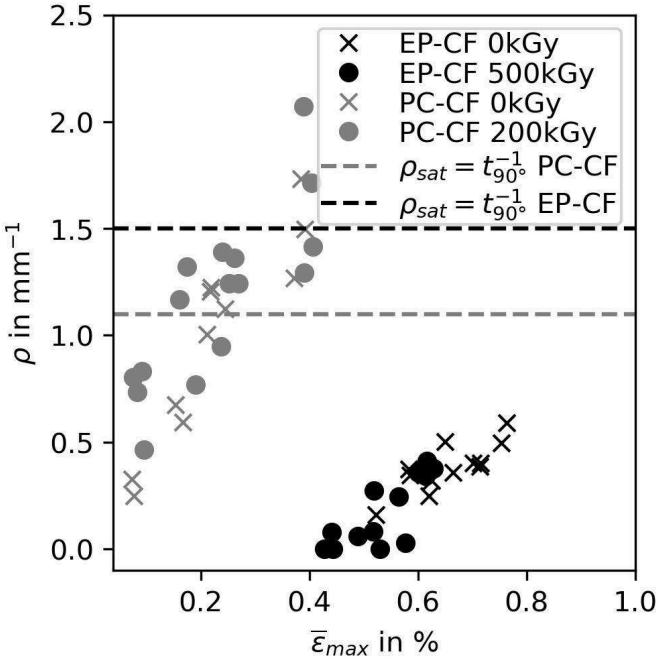

Figure 7: Crack density as a function of average maximum strain evaluated during the load controlled test

From the in-situ observation on a polished edge during loading, it became evident that especially glass fiber reinforced epoxy resin (EP-GF) and carbon fiber reinforced polycarbonate (PC-CF) tend to show cracking and debonding already during the first loading cycle. Especially in PC-CF tapes, numerous dry spots acted as crack incubators. A detailed analysis of these cracking sites revealed that due to self-filtration during impregnation dry spots are surrounded by areas with especially high fiber volume content. The strains to onset cracking are in the frequently mentioned strain limit of 0.3% [3] for both EP-CF (ε ~0.4 %) and PC-CF (ε <0.1 %) (see also Figure 7). For carbon fiber reinforced epoxy resin (EP-CF) the strains to onset cracking are higher as can be seen from the evaluation of the crack density after 10^5 cycles as a function of the average maximum strain evaluated by an extensometer during the load controlled tests in Figure 7. Only PC-CF and EP-CF could be evaluated regarding their crack density because in EP-GF cracks and debonds closed after unloading and were only visible during loading by strain evaluation on the polished edge (DIC). Hence, no representative area along the specimen's edge could be evaluated. By this evaluation, it becomes possible to generate an in-situ S-N curve based on homogenized elastic properties and local strains at crack initiation sites [2]. In this way, it was possible to identify the crack initiation sites as highly stressed fiber rich regions. Crack initiation was reproducible across all investigated laminates despite the molecular modification state but still specific to EP-GF, EP-CF and PC-CF. Hence, the micro- and mesoscopic structure

was identified as a potential source for uncertainty and deviation between predictions based on coupon level results and subcomponent testing results. It appears likely that inhomogeneity on these levels exist in larger components, e.g. as a result of local compaction [4], [5]. No-growth criteria like the frequently mentioned strain limit appear justified, considering the fact that cracking is often present in the first loading cycle and needs to be contained rather than avoided altogether. At the same time, the influence of local inhomogeneity requires a detailed understanding of local conditions to reduce uncertainty between the different analysis levels.

A major effort was spent in characterizing the polymer changes introduced by irradiation treatment. The experimental program placed a high emphasis on capturing the actual polymer response as part of a composite by replicating the conditions (e.g., triaxiality). It can be summarized that both polycarbonate and epoxy resin degrade as a result of irradiation exposure. However, from a range of experiments (on neat polymer) including uniaxial and triaxial loading, fatigue loading, relaxation and crack propagation, it was found that primarily those properties/ results reflecting the loading conditions within the laminate sufficiently could be correlated with the damage formation within the laminate. As an example, polycarbonate's tendency for crazing as precursor for cracking was found only for prolonged loading or a triaxial stress state. This effect also became evident by a higher crack density ρ of irradiated PC-CF laminates. In contrast to this, EP-CF laminates show an inverted effect of irradiation exposure because a reduced fracture toughness of the polymer did not translate into a higher crack density. However, an additional investigation of residual stresses revealed that these had been reduced by the irradiation exposure [6]. This unintended effect appears as a likely explanation.

To conclude the polymer effect on the fatigue crack initiation, it was found that it is of utmost importance to consider a broad range of properties that could potentially be affected by any alterations of the polymer. Partial investigations can easily be misleading. Special emphasis should be placed on the properties most relevant when a polymer is part of a laminate, namely, highly constrained loading conditions and fatigue crack resistance at crack incubation sites like debonds or dry spots.

Acknowledgement

This work was supported by the Deutsche Forschungsgemeinschaft (DFG, German Research Foundation) as part of the project "Correlation of matrix properties to the fatigue behavior of fiber reinforced polymers" – 468045930.

References

[1] Society of Automotive Engineers and National Institute for Aviation Research (U.S.), Eds., *Composite Materials Handbook Volume 1 - Revision G*. Warrendale, Pa.: SAE International on behalf of CMH-17, a division of Wichita State University, 2012.

[2] A. Baumann, M. Duhovic, and J. Hausmann, “In Situ Microscopy of Fatigue-Loaded Embedded Transverse Layers of Cross-Ply Laminates: The Role of an Inhomogeneous Fiber Distribution,” *J. Compos. Sci.*, vol. 8, no. 9, p. 366, Sep. 2024, doi: 10.3390/jcs8090366.

[3] A.J. Davies, Q. Qineti, and P. T. Curtis, “Fatigue in aerospace applications,” in *Fatigue in composites: science and technology of the fatigue response of fibre-reinforced plastics*, B. Harris, Ed., Boca Raton: CRC Press, 2003.

[4] A. Endruweit, F. Gommer, and A. C. Long, “Stochastic analysis of fibre volume fraction and permeability in fibre bundles with random filament arrangement,” *Composites Part A: Applied Science and Manufacturing*, vol. 49, pp. 109–118, Jun. 2013, doi: 10.1016/j.compositesa.2013.02.012.

[5] A. Zaami, I. Baran, Ton. C. Bor, and R. Akkerman, “Optical characterization of fiber-reinforced thermoplastic tapes for laser-based composite manufacturing,” *Composites Part A: Applied Science and Manufacturing*, vol. 146, p. 106402, Jul. 2021, doi: 10.1016/j.compositesa.2021.106402.

[6] A. Baumann and J. Hausmann, “Effect of high-energy radiation on the relaxation of residual stresses in Polycarbonate and Epoxy resin by stress optics,” *Radiation Physics and Chemistry*, Jan. 2025, doi: 10.1016/j.radphyschem.2024.112236.